Hindawi
Shock and Vibration
Volume 2021, Article ID 8819463, 12 pages
https://doi.org/10.1155/2021/8819463

Research Article

Combustion of Low-Concentration Gas in a Porous Media Burner: Reactor Design and Optimization

Jinhua Chen,[1,2] **Guangcai Wen**,[1,2] **Yanqing Li**,[3] **Xiangyun Lan**,[1,2] **Song Yan**,[3] **and Gang Wang**[4,3]

[1]*State Key Laboratory of the Gas Disaster Detecting Preventing and Emergency Controlling, Chongqing 400037, China*
[2]*China Coal Technology Engineering Group, Chongqing Research Institute, Chongqing 400037, China*
[3]*Shandong University of Science and Technology, College of Mining and Safety Engineering, Qingdao 266590, China*
[4]*Shandong University of Science and Technology, Mine Disaster Prevention and Control Ministry of State Key Laboratory Breeding Base, Qingdao 266590, China*

Correspondence should be addressed to Jinhua Chen; cqchenjinhua@126.com

Received 9 September 2020; Revised 21 October 2020; Accepted 18 May 2021; Published 26 May 2021

Academic Editor: M.I. Herreros

In order to utilize the low-concentration gas directly discharged into the atmosphere from 1.1% to 1.50% in coal mine production, the heat storage and oxidation equipment of gas was improved, and the heat storage and safety of gas under high-temperature environment were tested. The experimental results show that the regenerative oxidation system could provide a high-temperature oxidation environment of 1000°C for gas oxidation after changing the heating mode and enhancing the sealing property. The pressure curves of air and gas in the burner were similar. With the increase of gas concentration, the pressure difference between inlet and outlet tended to increase linearly with a minimum pressure differential of 4 kPa (air) and a maximum pressure differential of 11 kPa (1.50% gas). The internal pressure was relatively stable without an instantaneous pressure surge or explosion. The result of this study provides a reference for further research on the low-concentration gas regeneration oxidation unit at high temperatures.

1. Introduction

With the development of the coal mining industry, a large amount of unusable low-concentration gas is discharged into the air every year, causing serious greenhouse effect and waste of resources [1–5]. With the acceleration of the international community to deal with climate change, how to deal with low-concentration gas to reduce greenhouse gases has become an urgent problem [6–8].

Since conventional combustion cannot deal with low-concentration gas, it is a promising and effective measure to recycle low-concentration gas by regenerative oxidation equipment [9–15]. The conversion efficiency of methane by regenerative oxidation equipment is affected by many factors. The latest research shows that the heat recovery efficiency increased linearly with the increase of intake air flow rate and increased parabolically with the increase of intake methane concentration. However, the conversion rate of methane decreased with the increase of cycle period and inlet velocity [10, 12, 16]. In addition, the design, size, and materials of the equipment can influence the conversion rate of methane [17–19]. Therefore, many factors should be considered comprehensively to promote the conversion of low-concentration methane and improve the efficiency of heat recovery [20].

The temperature required for low-concentration gas oxidation is higher, but as the temperature increases, uneven temperature distribution will occur in the combustor cavity where the regenerative oxidation reaction occurs [21]. Lan [11] used the finite volume method to find that the uneven temperature distribution was related to the intake air flow rate, intake methane concentration, and cycle time. Gosiewski [21, 22] believed that the design parameters would also lead to the phenomenon of temperature heterogeneity

and analyzed it from the perspective of the algorithm and control system. Chen [18] used computational fluid dynamics simulation and concluded that the combustor size of high-temperature oxidation was the key factor determining the combustion stability of the system. At the same time, the heat accumulator would be damaged by the unevenly distributed high temperature in the combustor. Through experiments and finite element simulation studies, Liang [23] found that the thermal storage ceramic made of mullite would break at the supporting defects, and the method of using dense pillars could significantly enhance its resistance to damage. Srikanth [24] studied the heat storage performance of mullite and chromite, respectively. The simulation results showed that the thermal storage ceramics made of mullite and chromite exhibited good heat storage performance, among which the honeycomb ceramics based on chromite exhibited a longer heat storage time. Yuan's [25] simulation study showed that the square open-hole regenerator had a higher ground energy recovery than the hexagonal open-hole regenerator.

The above scholars studied the conversion efficiency of low-concentration gas and the temperature uniformity in the regenerative oxidation equipment from different aspects, which provided important reference for understanding the heat storage oxidation of low-concentration gas at high temperatures. However, they did not use mine gas according to the actual situation in the research. When the temperature reaches 1000°C, there is still a risk of explosion.

Therefore, the design and improvement of heat storage oxidation equipment are investigated in this work. At 1000°C, 1.1–1.5% of the heat storage capacity of the mine gas measuring reactor was used, as well as the pressure inside the reactor and the inlet and outlet of the gas. The safety of low-concentration gas regenerating and the oxidizing device was verified in order to provide a reference for the design of similar low-concentration gas regenerating and oxidizing device.

2. The Overall Design of Gas Regenerative Oxidation Equipment

The low-concentration gas thermal oxidation system consists of an inlet/exhaust system, a combustor, and a monitoring system. It can achieve low-gas thermal oxidation, release heat, and monitor reactions (see Figure 1). The combustor is the core part of the equipment.

2.1. Combustor. The combustor is the core device of the system and the main place where the low-concentration gas undergoes a regenerative oxidation reaction. Its main body is composed of five parts, namely, thermal storage ceramics, inner cylinder, thermal insulation layer, outer cylinder, and pedestal (see Figure 2).

When the low-concentration gas is subjected to regenerative oxidation, the lower the concentration, the higher the required temperature [26]. In order to oxidize the gas with a concentration of 0.8% to 1.5%, the combustor temperature should not be lower than 800°C [27]. The combustor is improved on the basis of Song Zhengchang's [28] design, with the addition of thermal storage ceramics. The mullite ceramics are preheated by electric heating and connected to a more modern monitoring system.

In the combustor cavity, high-temperature resistant tetragonal corundum mullite is used as the thermal storage ceramic. The monolithic ceramic diagram is shown in Figure 3, and the monolithic ceramic parameters are shown in Table 1. The honeycomb ceramic is fixed in the inner cylinder by refractory cement, and the gap between the ceramic and the refractory brick is filled with refractory cement to ensure that the gas in the combustor can only pass through the ceramic hole.

The inner cylinder is made of high-temperature resistant alloy steel 1Cr18Ni25Si, in which the long-term heat resistance temperature can reach above 1200°C. The insulation barrier is constructed from ceramic fiberboard and high-aluminum ceramic fiber material with a design thickness of 350 mm. The outermost layer is composed of steel, which can ensure that the surface temperature of the equipment is less than 50°C. The specific parameters are shown in Table 2. An electric heater is arranged in the inner cylinder wall composed of refractory bricks for heating ceramics. Seven temperature sensors are arranged on the left side of the combustor, while two pressure sensor interfaces are arranged on the right side. The temperature and pressure signals are processed by the data collector and displayed on the computer of the remote console.

2.2. Inlet/Exhaust System. The air inlet/exhaust system consists of a gas cylinder, high-precision gas flow controller, flame arrester, valves, and other auxiliary equipment, as shown in Figure 1. The gas cylinder provides the gas source and original power for system. A high-precision gas flow controller is used to monitor and control the gas flow. The flame arrester is installed at the front of the combustor to prevent the flame from passing back after the gas explodes in the combustor. Water-cooled sections are set at the front and rear ends of the combustor to prevent high temperatures from being transmitted to the system and damage the front and rear instruments. Remotely controllable solenoid valves, safety valves, and flow controllers ensure the safety of the system.

2.3. Monitoring System. Due to the high test temperature, there is a risk of explosion. To ensure the safety of test operators, this test uses a monitoring system to achieve remote operation and data recording. The monitoring system mainly includes components such as a camera, PID control system, high-speed data acquisition card, and gas analyzer. The main function is to control the solenoid valve switch, control the flow setting of the high-precision flow controller, and record the test phenomenon and test temperature, pressure, and other data.

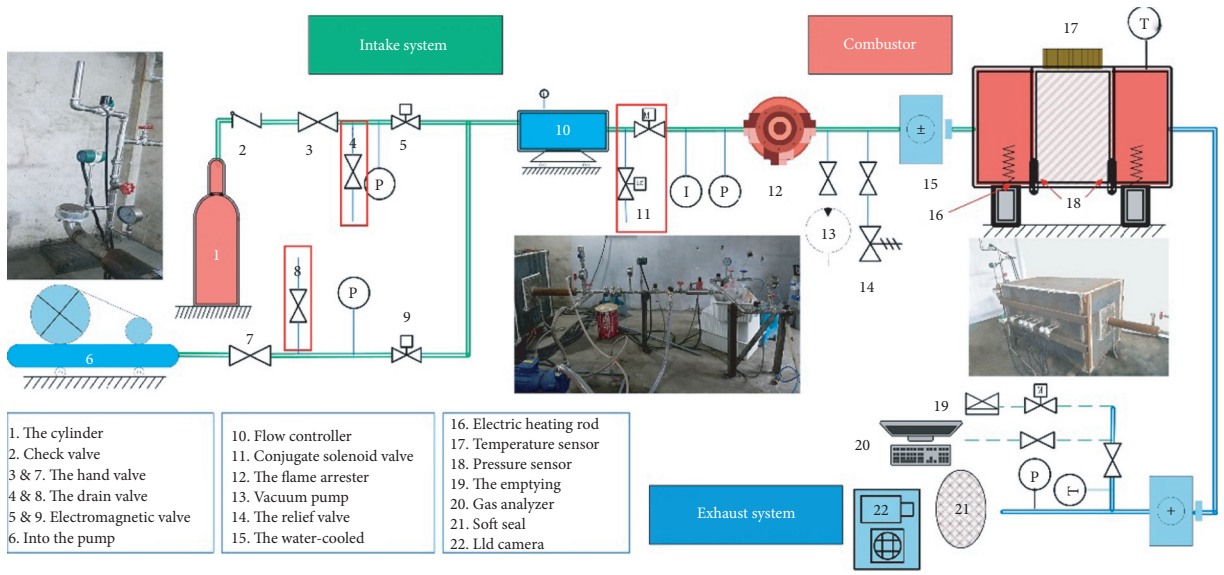

Figure 1: Regenerative oxidation equipment diagram.

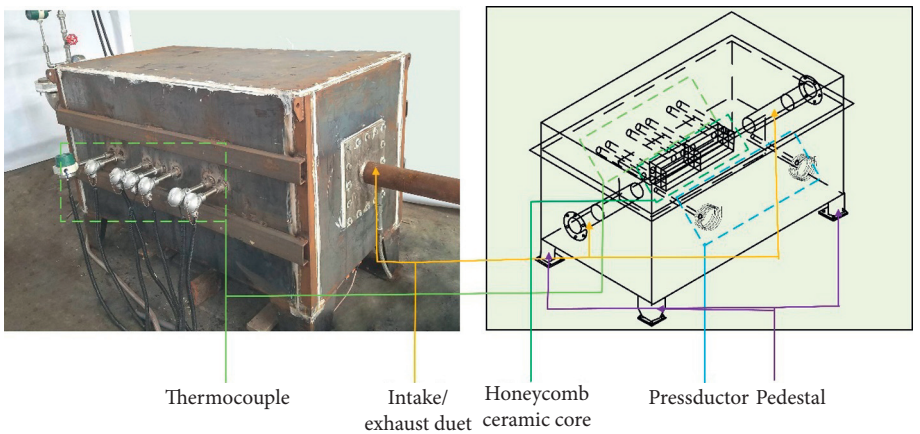

Figure 2: Combustor physical and structural diagram.

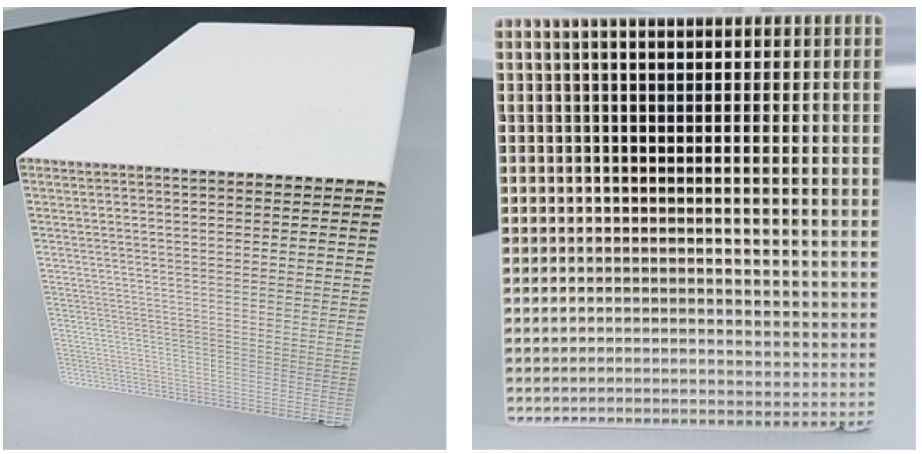

(a) (b)

Figure 3: Thermal storage ceramic diagram. (a) Monolithic ceramics. (b) Section diagram of monolithic ceramics.

Table 1: Monolithic ceramic parameters.

Dimension (length, width, and height) (m)	Single pore side length (m)	Number of pores	Pore surface area (m^2)	Mass (kg)
$0.15 \times 0.15 \times 0.3$	$e = 0.03$	40×40	5.8	5.71
Volume (m^3)	**Single pore side thickness (m)**	**Porosity**	**Specific surface area (m^2/m^3)**	**Heating up to 1000°C required energy (kJ)**
0.00675	$a = 0.00075$	65%	859	10352

Table 2: The parameter table of the combustor.

Type	Inner cylinder	Outer cylinder
Diameter	φ105 mm × 0.5 mm	φ300 m × 6 mm
Height	300 mm	300 mm
Material	Alloy steel 1Cr18Ni25Si	Stainless steel #304
Filling material	Ceramic heat storage body	Ceramic fiberboard and the high-aluminum ceramic fiber material
Filling height	120 mm	300 mm
Filling position	60 mm from the bottom	Inner cylinder peripheral

3. Testing of Gas Regenerative Oxidation Equipment

3.1. Theoretical Analysis of Combustor Feasibility. As the main site of low-concentration gas oxidation reaction, the combustor is the key part of the equipment. Therefore, it is necessary to analyze the length of the honeycomb ceramics in the combustor and the temperature in the combustor chamber to ensure that a fixed volume of gas reaches the oxidation temperature after entering.

(1) Determine the length of honeycomb ceramics. The combustor relies on high-temperature ceramics to heat methane for high-temperature heat storage. Assuming the target temperature is 1100°C, the length of the ceramic segment is calculated as follows:

The natural convection heat transfer coefficient of air is 5–25 W/m^2K, and its forced convection heat transfer coefficient is 20–100 W/m^2K. Assume air convective heat transfer coefficient and ceramic preheating temperature are $h = 20\ W/m^2K$ and$t_0 = 1100$°C, respectively. In the following equations, S, c, and q_m represent the cross-sectional flow area of ceramic, the average specific heat of air, and air mass flow rate, respectively. A calculus method is employed to estimate the length of the required thermal storage ceramics L [27].

Taking a microelement dx along the ceramic radial, the temperature rises from t to t' (see Figure 4); then:

$$\text{Ceramic heat transfer: } Q = hA(t_0 - t) = hSd_x(t_0 - t), \quad (1)$$

$$\text{Gas heat absorption: } Q_{\text{absorption}} = cq_m d_t, \quad (2)$$

$$\because Q = Q_{\text{absorption}}, \quad (3)$$

$$\therefore hSd_x(t_0 - t) = cq_m d_t, \quad (4)$$

$$\therefore hSd_x = \frac{cq_m d_t}{1100 - t}. \quad (5)$$

With integration on both sides of the equation,

$$\int_0^L hSd_x = \int_0^{1000} \frac{cq_m d_t}{1100 - t}, \qquad \therefore \text{hSL} = cq_m \ln(1100 - t)\big|_{1000}^{0}. \quad (6)$$

The formula calculated by substituting the data is as follows:

$$L = \frac{cq_m}{hS} \ln \frac{1100}{100} = \frac{1.074 \times 0.035 \times \ln 11}{20 \times 0.15 \times 0.15 \times 0.65} = 0.3004\ \text{m}. \quad (7)$$

It can be seen from the above calculation process that the thermal storage ceramic with a length of 0.3 meters can heat the gas temperature to a preset temperature of 1100°C. Therefore, placing two pieces of ceramic with a length of 0.3 meters in the combustor can theoretically heat the combustor to 1000°C.

(2) Determine the temperature in the combustor cavity after the mixed gas. After 1 L, gas with low concentration at 20°C enters the high-temperature field (the preheating temperature is 1100°C); whether the oxidation temperature can be reached in a very short time is related to the smooth operation of the high-temperature regenerative oxidation equipment with low-concentration gas. Now the theoretical analysis is carried out to determine whether the target temperature can be reached.

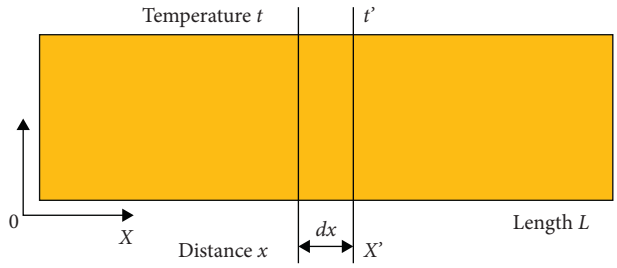

Figure 4: Calculus schema.

The first step is to determine the amount of residual air matter in the combustor chamber. The volume in the chamber of the combustor is 8 L. It is assumed that the pressure and volume do not change after the air is heated to 1000°C at 20°C. When low-concentration gas enters the chamber, the amount of matter in the chamber will change, and then the mass of matter remaining in the chamber can be calculated as follows.

According to the ideal gas equation,

$$PV = nRT. \tag{8}$$

Assuming no change in pressure and volume,

$$n_1 RT_1 = n_2 RT_2. \tag{9}$$

The molar mass of air is 29 g/mol. The air density at 20°C is 1.205 kg/m^3, and 1.205 g/L is taken. Then n_1, the quantity of 8 L of air substance at 20°C, is

$$n_1 = \frac{\rho v}{M_A} = \frac{1.205 \times 8 \times 0.001 \times 1000}{29} = 0.3324\,\text{mol}. \tag{10}$$

Therefore, the amount of residual air matter in the high-temperature field is

$$n_2 = \frac{n_1 T_1}{T_2} = \frac{0.3324 \times 293}{1473} = 0.0661\,\text{mol}. \tag{11}$$

When a high-temperature object emits heat to a low-temperature object, the temperature of the high-temperature object will decrease while the temperature of the low-temperature object will increase. This process must be carried out until the temperature of the two objects is equal, that is, until the two objects reach the thermal equilibrium state. In the case of heat loss, the heat released by high-temperature objects is equal to the heat absorbed by low-temperature objects [29].

After entering the chamber, the low-concentration gas at 20°C will exchange heat with the high-temperature air in the room until it reaches the state of thermal equilibrium. It is assumed that, in this process, the heat released by the high-temperature gas is equal to the heat absorbed by the low-temperature gas. Suppose the thermal equilibrium temperature after mixing two different temperatures of air is T with an initial temperature of high-temperature air T_2 of 1100°C and a mass ofM_{n2}. The initial temperature of low-temperature air T_1 is 20°C and a mass of M_{n1}, and the equilibrium temperature after heat exchange can be calculated by the following calculation.

High-temperature gas emits heat:

$$Q_{\text{emit}} = CM_{n2}(T_2 - T) = Cn^2_{\text{remaining}} M_A (T_2 - T). \tag{12}$$

Low-concentration gas absorption temperature is as follows:

$$Q_{\text{absorption}} = CM_{n1}(T - T_1) = Cn^1_{\text{initial}} M_A (T - T_1). \tag{13}$$

By $Q_{\text{emits}} = Q_{\text{absorption}}$, the mixing temperature can be calculated.

$$n^2_{\text{remaining}}(T_2 - T) = n^1_{\text{initial}}(T - T_1),$$

$$0.0661 \times (1100 - T) = \frac{\rho v}{M_A}(T - 20) = \frac{1.205 \times 0.001 \times 1000}{29} \times (T - 20). \tag{14}$$

$T = 682.8$°C.

Therefore, the equilibrium temperature reached by heat exchange after gas with low concentration at 20°C enters the high-temperature oxidation chamber is 682.8°C.

The heating power of the combustor is 35 kW, and the combustor is well sealed without heat loss. Assuming that the time from gas entry to reaction is 30 ms (intake 20 ms, reaction 10 ms), the heat provided by the combustor through the heating element for the gas can be calculated as follows.

The total mass of the mixed gas is

$$M_{\text{total}} = n^2_{\text{remaining}} M_A + n^1_{\text{initial}} M_A = 0.0661 \times 29 + 1.205 \times 0.001 \times 1000 = 3.1219\,\text{g}. \tag{15}$$

The specific heat capacity of air is 1030 J/(kg·°C), and the heat absorbed is

$$Q_{\text{absorption}} = Wt = 35 \times 1000 \times 30 \times 0.001 = 1050\,\text{J}. \tag{16}$$

The temperature increase after mixing is

$$Q_{\text{absorption}} = CM_{\text{total}} \Delta T, \tag{17}$$

$$\Delta T = \frac{Q_{\text{absorption}}}{CM_{\text{total}}} = \frac{1050}{1030 \times 3.1219 \times 0.001} = 326.5. \tag{18}$$

Therefore, the temperature will rise by 326.5°C after heating through the heating element.

Since heat exchange and combustor heating are carried out at the same time, it can be concluded that the temperature of low-concentration gas after heat exchange and heating element heating is $T_{\text{total}} = 682.8 + 326.5 = 1009.3$°C. Therefore, the low-concentration gas at 20°C can be heated up to 1000°C within 30 ms after entering the combustor chamber, and the equipment can perform high-temperature regenerative oxidation of low-concentration gas.

3.2. Experimental Design. In order to test whether the low-concentration gas regenerative oxidation equipment has the ability to quickly heat up to 1000°C, the regenerative oxidation equipment heat storage capacity test was performed after the first packaging.

In the preparation stage of the test, the tester shall ensure that there are no inflammable and explosive articles around the test system. The pipelines, valves, and instruments were examined to confirm the safety. In addition, airtightness inspection should be performed. During the test phase, the power supply and the monitoring system should be turned on first to provide pure air to purge the test system. After five minutes, the cooling water was turned on. Then the honeycomb ceramic was preheated to 200°C, and the temperature was set to the test temperature (the maximum temperature is 1100°C). The ceramic temperature should be maintained for 10 minutes after reaching the set value. Finally, the vacuum pump in the tester and the solenoid valve linkage mode were turned on. In addition, the tester recorded the test phenomenon of the soft seal end and measured the exhaust gas composition. At the end of the test, the equipment was turned off by following equipment instructions of the tester to ensure that the methane concentration in the surrounding air is less than 0.5%. The flowchart of the test operation is shown in Figure 5.

4. Discussion of Results

4.1. Preheating Process of the Combustor. After the combustor is designed and packaged, it is necessary to conduct warm-up debugging so that problems can be found and corrected in time, to prevent problems caused by equipment that is not properly designed, to avoid safety accidents, and to ensure the availability and safety of the device. In the preheating process of the combustor, the following three issues were found and modified.

(1) The heating rod overheated and fused. During the preheating of the combustor, when the temperature raised to 650°C, the system alarmed us promptly. After stopping the preheating, the inspection found that all three groups of heating rods were broken (see Figure 6).

The test uses 304 stainless steel (0Cr18Ni9), which can withstand a high temperature of 800 °C but fuse at 650 °C. The dismantling analysis of the combustor and the reasonable causes for the fracture are assumed. When the electric heating rod is close to the ceramic wall surface, the heat transfer efficiency is low, which causes the local temperature of the heating rod to be too high in a narrow space, reaching the melting point of the heating rod and causing the electric heating rod to melt.

According to the assumption that the heating rod is fused, the combustor is improved. Continuously cut small holes on the ceramic wall close to the heating rod were performed to promote the diffusion of heat, increase the space around the heater, and prevent the heating rod from melting due to excessive concentration of the temperature around the heater. At the same time, the electric heating rod is replaced with austenitic chromium-nickel stainless steel with a melting point of 1470°C, which has better heat resistance [30]. After heating and debugging, it was determined that the problem of heating rod fusing was solved.

(2) The temperature of the honeycomb ceramics is not uniform. The test system uses high-temperature electric heating rods to transfer heat to the honeycomb ceramics. The advantage of this type of electric heating honeycomb ceramics is the high-temperature controllability. The temperature during the test can be controlled to 1°C above and below the set temperature. After several preheating tests, it was found that although the average temperature of the ceramic can reach 1000°C, there are several cases where the temperature distribution of the honeycomb ceramic is uneven in the horizontal and vertical directions (see Figure 7). By dismantling the furnace and checking the heating of the ceramic, it was found that the side of the ceramic was sintered, and there were not many ceramic holes with obvious heating marks on the inner wall of the ceramic.

This is because the heat is transferred to the ceramic interior layer by layer through the ceramic sidewall, and the porous ceramic thin-wall structure significantly obstructs the heat transfer, resulting in the difficulty of ceramic interior temperature rise [31]. Therefore, on the basis of the original approach, the equipment increases the way of hot air sweeping to heat the ceramics so as to ensure the uniformity of the internal temperature of heat-storage honeycomb ceramics. After the improvement, it was found that the internal heating of ceramics was basically uniform through furnace removal inspection.

(3) *Poor Sealing*. The tightness of the combustor will affect the stability and uniformity of the chamber temperature. The chamber of the combustor is made of refractory brick, and the brick joints are sealed with imported fireproof cement. During the test, the local temperature of the firebrick is usually above 1000°C, and the frequent heating and cooling operation make the fireproof cement easy to dry and crack, leading to the complete failure of the inner cavity of the combustor to meet the test sealing requirements.

In order to solve the problem of poor sealing performance of the inner cavity of the combustor, the inner cavity of the combustor is changed into a steel tube, which is easier to be sealed. At the same time, all bolts, steel plate connections, and sensor connections of the combustion chamber should be sealed with glass glue. The interface of the heating

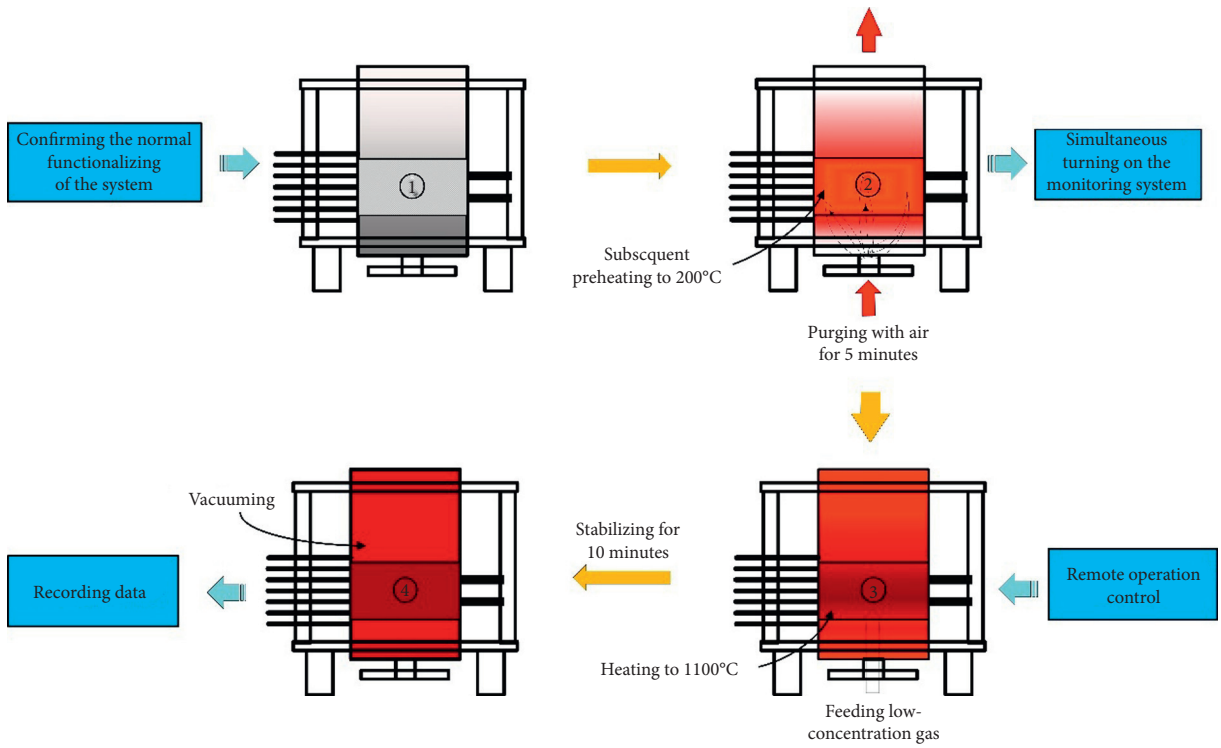

Figure 5: Operation steps of temperature rise test diagram.

Figure 6: Fusing diagram of the heating rod.

rod should be covered and sealed with a sealing cover at the bottom, which can prevent the steel from transferring heat to the air.

4.2. Temperature Rise Test of Heat Storage Oxidation Equipment. According to the above heating test step, the heating test was performed to obtain the heat storage capacity evaluation data of four groups of low-concentration gas high-temperature regenerative equipment. The results are as follows.

Figure 8 shows the correlation diagrams of four sets of test temperatures with target temperatures and the average temperatures at 800°C, 900°C, 1000°C, and 1050°C. In Figure 8, Test, Set Temp, and Ave Temp represent four testing groups, the target temperature, and the average temperature of the four sets of temperatures, respectively. It can be seen that the average temperature obtained in the experiment is basically consistent with the target temperature. The deviation was only 6% when the target temperature was 800°C, which is within 1% and meets the experimental requirements. Therefore, it can be concluded that the combustor has

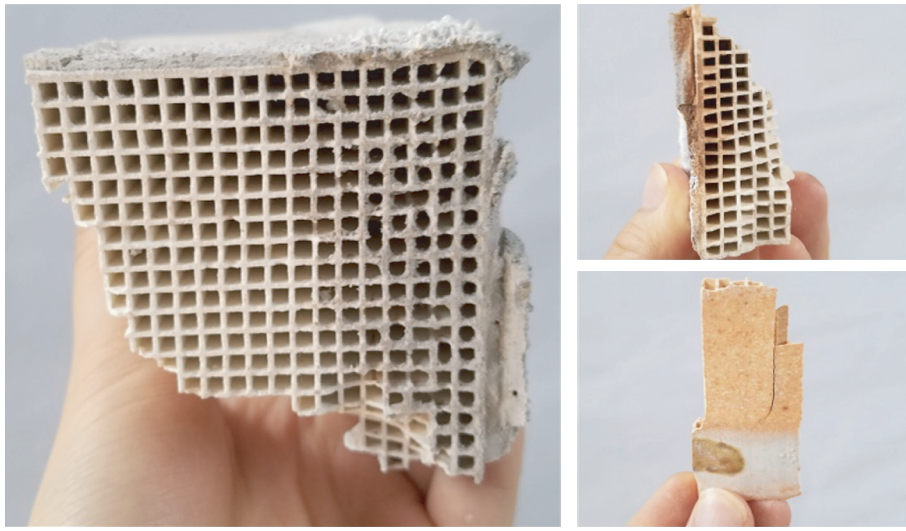

Figure 7: Effect picture of ceramics after heating.

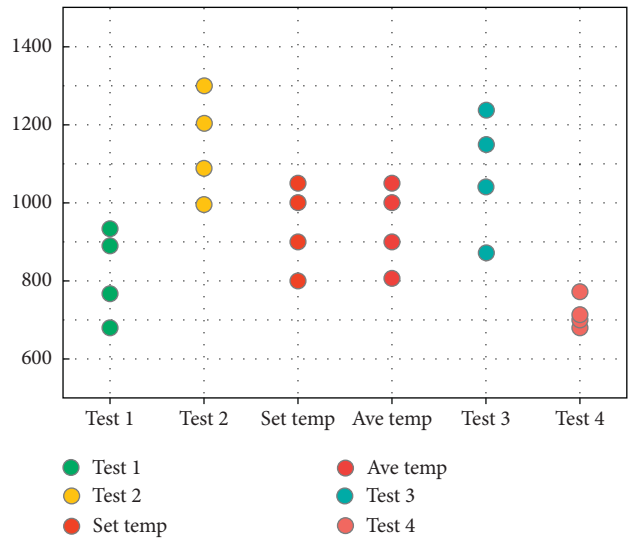

Figure 8: Relationship between experimental data and target temperature.

optimal heat storage capacity and can provide equipment support for low-concentration gas regenerative oxidation. In addition, the experimental data varied from 650°C to 1200°C and concentrated in the range of 800°C to 1100°C, which can provide heat storage performance and ensure safety.

Based on Figure 8, the relationship between average temperature and heating time is further analyzed. It can be seen from Figure 9 that the heating time curve stays stable first and then rises. It takes 23 hours for the temperature to rise from room temperature to 800°C, but the time interval from 800°C to 900°C is negligible. This is because when the system heats up from room temperature to 800°C, the whole system needs to be heated, so the consumption time increases. From 800°C to 900°C, the system can heat up rapidly because it has already been heated. It takes 5 hours for the combustor to heat up from 900°C to 1000°C. According to the curve trend in the figure, it takes about 4–6 hours to heat up from 1000°C to 1100°C. This may be because the system is in a transition period from the end of preheating to cyclic stability when the oxidation of methane accompanies the operation of the combustor. When the combustor is in operation, the temperature of the boundary will continuously rise. Therefore, the heat loss to the surrounding environment will increase, and the heat cannot be trapped in the combustor chamber. At the same time, as the increase of methane intake concentration will reduce the temperature in the combustor chamber, if the intake concentration is properly adjusted according to the real-time temperature feedback from the monitoring system, the heating time can be shortened [32–34].

Based on the above results, it can be seen that the low-concentration gas heat storage high-temperature oxidation equipment can better meet the requirements; that is, the average temperature can reach the set temperature in a relatively short time. In the meantime, the heating time will be significantly reduced after the cycle is stable, and the heating time will be stable for 4–6 hours when the temperature interval is set at 1000°C.

4.3. Low-Concentration Gas Oxidation Pressure Test. The air and gas concentrations of 1.10%, 1.20%, 1.30%, 1.40%, and 1.50% were measured when the air flow velocity was set at 400 L/min and the inlet pressure at 100 Kpa.

As can be seen from Figure 10, when the inlet pressure and outlet pressure are unchanged, the pressure change curves of inlet air and inlet gas are basically the same without significant difference. The peak value of the air pressure curve is due to the rapid expansion of the air after the restoration of ceramic temperature. However, with the increase of the amount of air entering, the expansion range is small, and the inlet and outlet pressure then return to normal. The curves of gas pressure at different concentrations are very similar. As the gas enters the high-temperature

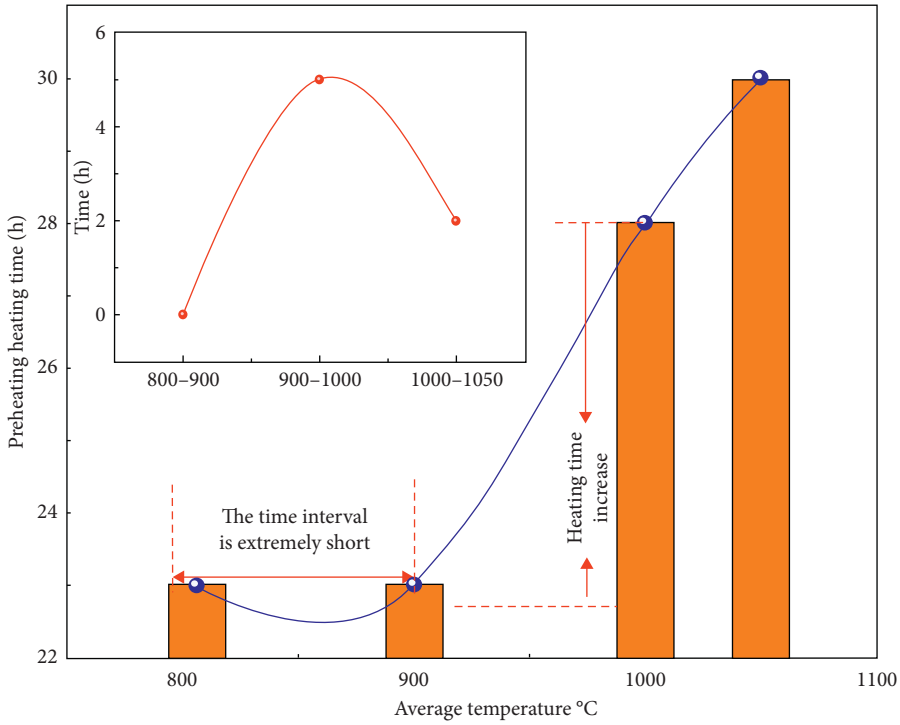

Figure 9: Relationship between average temperature and heating time.

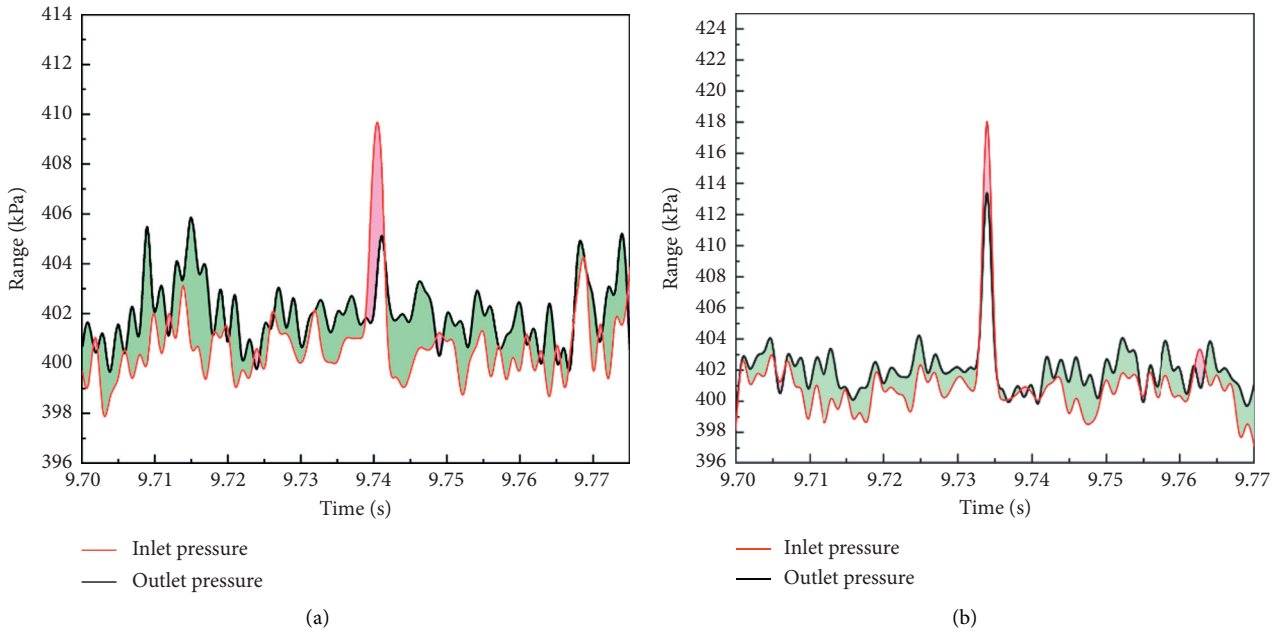

Figure 10: Continued.

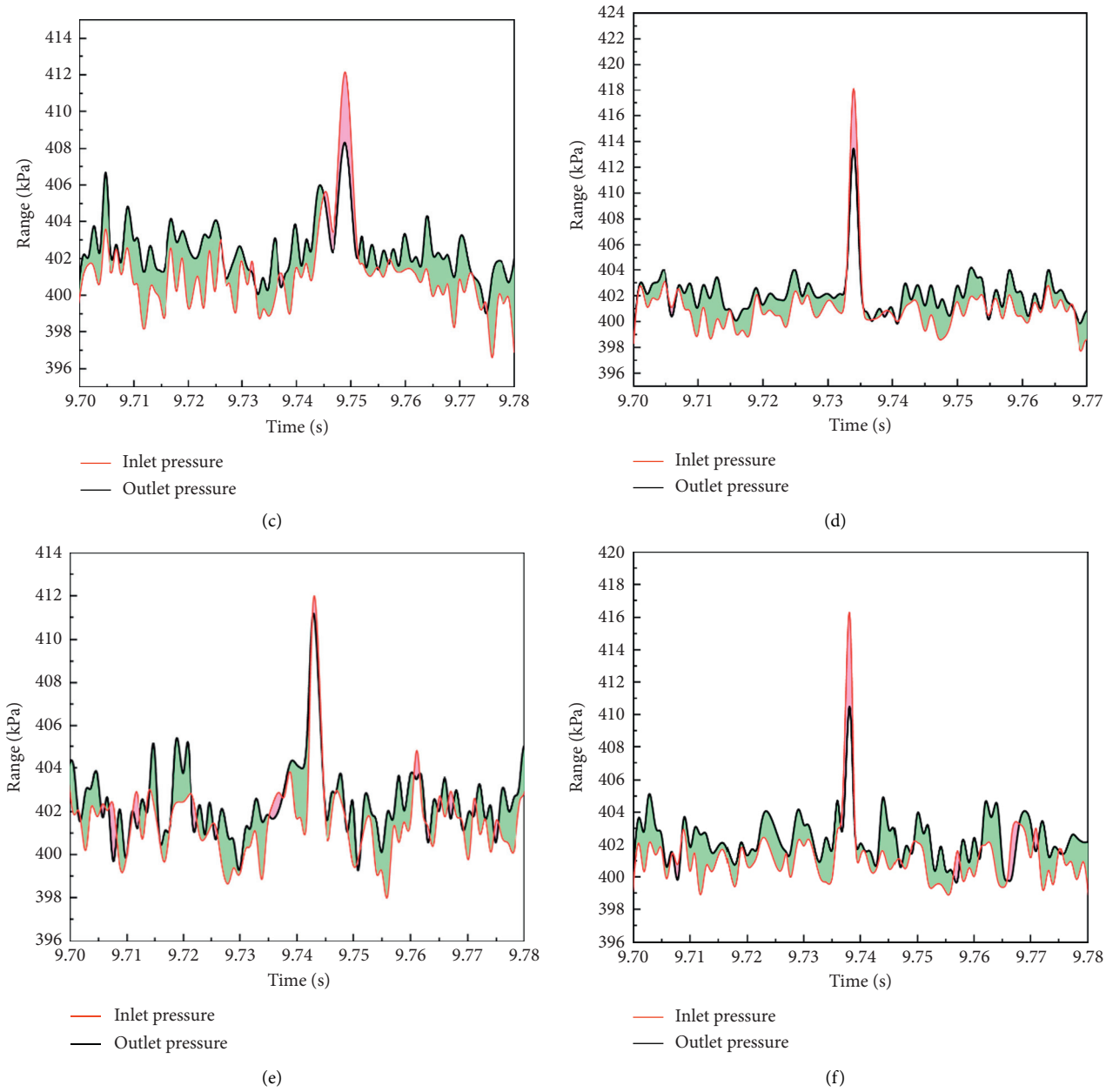

Figure 10: Experimental pressure detection charts (a), (b), (c), (d), (e), (f), and (g) show the pressures of air (a) and gas concentrations of 1.10%, 1.20%, 1.30%, 1.40%, and 1.50%.

environment of the burner, it is rapidly oxidized to carbon dioxide and water with releasing heat. Meanwhile, the gas becomes larger in volume while absorbing heat. The resulting carbon dioxide, however, mixes with water vapor and oxygen, which suppresses the pressure increase and causes it eventually to return to normal. The change range of inlet and outlet pressure is small, indicating that no sudden volume expansion and sharp pressure rise caused by oxidation reaction occurred in the reactor. Therefore, compared with the air, the gas mixing a small amount of carbon dioxide and water vapor has no substantial effect on the reaction process without a significant increase in pressure or an explosion in the instantaneous pressure jump.

Figure 11 shows the pressure difference between inlet and outlet. It can be seen that the pressure difference of air was small, indicating that the expansion volume of air when heated is small, and the explosion risk coefficient is low. With the increase of gas concentration, the pressure difference increased almost as a function. When the gas concentration was 1.5%, the pressure difference reached its maximum value of 11 Kpa, indicating that the trend of low-concentration gas passing through the hot heat source is close to the pressure peak. However, when the gas concentration increased from 1.1% to 1.5%, the pressure difference did not change significantly, indicating that there was no sharp pressure increase. When using low-

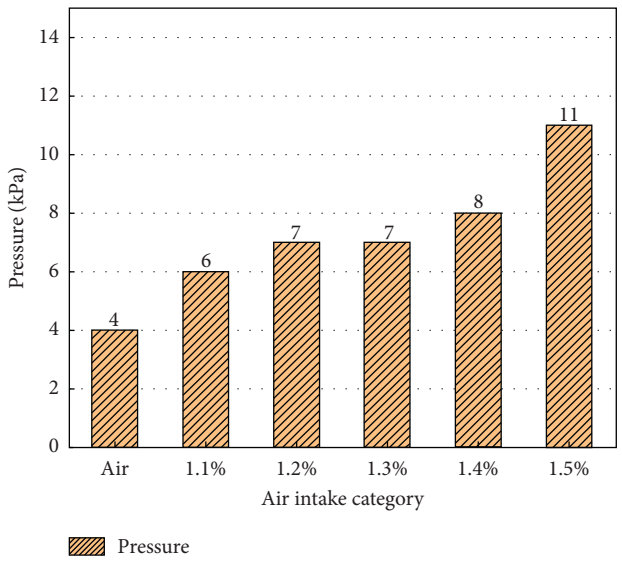

Figure 11: Pressure difference between inlet and outlet.

concentration gas in the mine in the future, the gas concentration can be controlled below 1.5% by mixing air so as to realize the safe and efficient utilization of low-concentration gas.

5. Conclusion

In order to improve the efficiency and safety of low-concentration gas regenerative oxidation equipment, we design and build a set of low-concentration gas high-temperature regenerative equipment in this work. The main conclusions of the analysis and discussion on the high-temperature heat storage capacity of the equipment are as follows:

(1) The burner is demonstrated to be feasible from a theoretical point of view.

(2) The burner was improved in terms of the heating mode and sealing, which can provide an oxidizing environment of 1000°C for the oxidation of low-concentration gas with an optimal heat storage capacity.

(3) When the gas concentration is 1.1%–1.5%, the pressure difference between the inlet and outlet is small, and the thermal storage oxidation system operates stably without an explosion caused by volume expansion. This result demonstrates that the gas concentration of 1.1%-1.5% is within the safe range, which provides guidance for low-concentration gas use.

Data Availability

The data used to support the findings of this study are available from the corresponding author upon request.

Conflicts of Interest

The authors declare that there are no conflicts of interest regarding the publication of this paper.

Acknowledgments

The authors would like to acknowledge the support of the "Thirteenth Five-Year" National Science and Technology Major Funding Project (Project no. 2016ZX05045-006-002), key projects supported by the Science and Technology Innovation and Entrepreneurship Fund of Tian Di Science and Technology Co., Ltd. (Project no. 2019-TD-ZD004), and key projects supported by China Coal Technology Engineering Group Chongqing Research Institute (Project no. 2018ZDXM06).

References

[1] A. Setiawan, E. M. Kennedy, and M. Stockenhuber, "Development of combustion technology for methane emitted from coal-mine ventilation air systems," *Energy Technology*, vol. 5, no. 4, pp. 521–538, 2017.

[2] X. Jiang, D. Mira, and D. L. Cluff, "The combustion mitigation of methane as a non-CO2 greenhouse gas," *Progress in Energy and Combustion Science*, vol. 66, pp. 176–199, 2018.

[3] A. Banerjee and A. V. Saveliev, "High temperature heat extraction from counterflow porous burner," *International Journal of Heat and Mass Transfer*, vol. 127, pp. 436–443, 2018.

[4] A. Banerjee and A. Saveliev, "Emission characteristics of heat recirculating porous burners with high temperature energy extraction," *Front Chem*, vol. 8, p. 67, 2020.

[5] X. Wang, K. Wei, S. Yan et al., "Efficient and stable conversion of oxygen-bearing low-concentration coal mine methane by the electrochemical catalysis of SOFC anode: from pollutant to clean energy," *Applied Catalysis B: Environmental*, vol. 268, 2020.

[6] J. L. Ellzey, E. L. Belmont, and C. H. Smith, "Heat recirculating reactors: fundamental research and applications," *Progress in Energy and Combustion Science*, vol. 72, pp. 32–58, 2019.

[7] S. A. Montzka, E. J. Dlugokencky, and J. H. Butler, "Non-CO2 greenhouse gases and climate change," *Nature*, vol. 476, no. 7358, pp. 43–50, 2011.

[8] X. Yang, F. Song, Y. Wu, Y. Zhong, and S. Xu, "Investigation of rotating detonation fueled by a methane-hydrogen-carbon dioxide mixture under lean fuel conditions," *International Journal of Hydrogen Energy*, vol. 45, no. 41, pp. 21995–22007, 2020.

[9] S. A. Ghoreishi-Madiseh, H. Kalantari, A. F. Kuyuk, and A. P. Sasmito, "A new model to analyze performance of mine exhaust heat recovery systems with coupled heat exchangers," *Applied Energy*, vol. 256, 2019.

[10] B. Lan, Y.-R. Li, X.-S. Zhao, and J.-D. Kang, "Industrial-Scale experimental study on the thermal oxidation of ventilation air methane and the heat recovery in a multibed thermal flow-reversal reactor," *Energies*, vol. 11, no. 6, 2018.

[11] B. Lan and Y.-R. Li, "Numerical study on thermal oxidation of lean coal mine methane in a thermal flow-reversal reactor," *Chemical Engineering Journal*, vol. 351, pp. 922–929, 2018.

[12] B. Zheng, Y. Liu, P. Sun, J. Sun, and J. Meng, "Oxidation of lean methane in a two-chamber preheat catalytic reactor," *International Journal of Hydrogen Energy*, vol. 42, no. 29, pp. 18643–18648, 2017.

[13] K. Gosiewski, A. Pawlaczyk, and M. Jaschik, "Thermal combustion of lean methane-air mixtures: flow reversal research and demonstration reactor model and its validation," *Chemical Engineering Journal*, vol. 207-208, pp. 76–84, 2012.

[14] K. Gosiewski and A. Pawlaczyk, "Catalytic or thermal reversed flow combustion of coal mine ventilation air methane: what is better choice and when?" *Chemical Engineering Journal*, vol. 238, pp. 78–85, 2014.

[15] A. H. Ibrahim, S. Y. Kamal, T. W. Abou-Arab, M. A. Nemitallah, M. A. Habib, and H. Kayed, "Operability of fuel/oxidizer-flexible combustor holding hydrogen-enriched partially premixed oxy-flames stabilized over a perforated plate burner," *Energy & Fuels*, vol. 34, no. 7, pp. 8653–8665, 2020.

[16] Z. Sang, Z. Bo, X. Lv, and Y. Weng, "Numerical investigations of the influencing factors on a rotary regenerator-type catalytic combustion reactor," *Catalysts*, vol. 8, no. 5, 2018.

[17] L. Huang, Y. Wang, S. Pei et al., "Effect of elevated pressure on the explosion and flammability limits of methane-air mixtures," *Energy*, vol. 186, 2019.

[18] J. Chen, W. Song, and D. Xu, "Optimal combustor dimensions for the catalytic combustion of methane-air mixtures in micro-channels," *Energy Conversion and Management*, vol. 134, pp. 197–207, 2017.

[19] A. Pawlaczyk and K. Gosiewski, "Combustion of lean methane-air mixtures in monolith beds: k," *Chemical Engineering Journal*, vol. 282, pp. 29–36, 2015.

[20] M. Mao, J. Shi, Y. Liu, M. Gao, and Q. Chen, "Experimental investigation on control of temperature asymmetry and nonuniformity in a pilot scale thermal flow reversal reactor," *Applied Thermal Engineering*, vol. 175, 2020.

[21] K. Gosiewski and A. Pawlaczyk-Kurek, "Impact of thermal asymmetry on efficiency of the heat recovery and ways of restoring symmetry in the flow reversal reactors," *International Journal of Chemical Reactor Engineering*, vol. 17, no. 3, 2019.

[22] K. Gosiewski, A. Pawlaczyk, and M. Jaschik, "Energy recovery from ventilation air methane via reverse-flow reactors," *Energy*, vol. 92, pp. 13–23, 2015.

[23] X. Liang, Y. Li, L. Pan et al., "Fracture behavior of mullite reticulated porous ceramics for porous media combustion," *Front Chem*, vol. 7, p. 792, 2019.

[24] O. Srikanth, S. D. Khivsara, R. Aswathi et al., "Numerical and experimental evaluation of ceramic honeycombs for thermal energy storage," *Transactions of the Indian Ceramic Society*, vol. 76, no. 2, pp. 102–107, 2017.

[25] F. Yuan, H. Wang, P. Zhou, A. Xu, and D. He, "Heat transfer performances of honeycomb regenerators with square or hexagon cell opening," *Applied Thermal Engineering*, vol. 125, pp. 790–798, 2017.

[26] C. Jing-kun, Z. Xin-lei, C. Shan-chang, L. Meng, L. Rui-feng, and S. Chun-yu, "Experimental study on high temperature oxidation of extremely low concentrations methane," *Clean Coal Technology*, vol. 18, no. 06, pp. 91–93+98, 2012.

[27] M. van Sint Annaland and R. C. Nijssen, "A novel reverse flow reactor coupling endothermic and exothermic reactions: an experimental study," *Chemical Engineering Science*, vol. 57, no. 22-23, pp. 4967–4985, 2002.

[28] S. zhengchang, L. baiquan, and Z. Shining, "Experimental study on the excess-enthalpy combustion of low concentration methane in ceramic foams," *Journal of China Coal Society*, vol. 36, no. 04, pp. 628–632, 2011.

[29] X. Cheng, X. Liang, and Z. Guo, "Entransy decrease principle of heat transfer in an isolated system," *Chinese Science Bulletin*, vol. 56, no. 9, pp. 847–854, 2011.

[30] K. Osozawa, K. Bohnenkamp, and H.-J. Engell, "Potentiostatic study on the intergranular corrosion of an austenitic chromium-nickel stainless steel," *Corrosion Science*, vol. 6, no. 9, pp. 421–433, 1966.

[31] S. Funayama, H. Takasu, S. T. Kim, and Y. Kato, "Thermochemical storage performance of a packed bed of calcium hydroxide composite with a silicon-based ceramic honeycomb support," *Energy*, vol. 201, p. 11, 2020.

[32] P. Rajpara, A. Dekhatawala, R. Shah, and J. Banerjee, "Thermal and emission characteristics of reverse air flow CAN combustor," *International Journal of Thermal Sciences*, vol. 128, pp. 175–183, 2018.

[33] W. Zuo, J. E, R. Lin, Y. Jin, and D. Han, "Numerical investigations on different configurations of a four-channel mesoscale planar combustor fueled by hydrogen/air mixture," *Energy Conversion and Management*, vol. 160, pp. 1–13, 2018.

[34] R. C. Zhang, X. Y. Huang, W. J. Fan, and N. J. Bai, "Influence of injection mode on the combustion characteristics of slight temperature rise combustion in gas turbine combustor with cavity," *Energy*, vol. 179, pp. 603–617, 2019.